DALTON
FULL PAPER

Half-sandwich complexes of molybdenum-(III), -(IV) and -(V) with P–O and P–N bifunctional ligands Ph_2PCH_2X (X = 2-oxazolinyl, or $C(O)NPh_2$)

Jean-Michel Camus,[a] Dolores Morales,[a] Jacques Andrieu,[a] Philippe Richard,[a] Rinaldo Poli,*[a] Pierre Braunstein[b] and Frédéric Naud[b]

[a] *Laboratoire de Synthèse et d'Electrosynthèse Organométalliques (UMR 5632 CNRS), Faculté des Sciences "Gabriel", Université de Bourgogne, 6 Boulevard Gabriel, F-21000 Dijon, France*
[b] *Laboratoire de Chimie de Coordination (UMR 7513 CNRS), Université Louis Pasteur, 4 rue Blaise Pascal, F-67070 Strasbourg Cedex, France*

Received 27th March 2000, Accepted 9th June 2000
Published on the Web 11th July 2000

The reaction of the ligands Ph_2PCH_2X (X = 2-oxazolinyl, **I**; or $C(O)NPh_2$, **II**) with the half-sandwich molybdenum(III) precursors $[Mo(\eta\text{-}C_5R_5)(\mu\text{-}Cl)_2]_2$ (R = H or Me) has been investigated. Ligand **I** reacts with both complexes to form the corresponding adducts $[Mo(\eta\text{-}C_5R_5)Cl_2(Ph_2PCH_2C_3H_4NO)]$ (R = H, **1**; or Me, **2**). The reaction between **I** and $[MoCp^*Cl_4]$ ($Cp^* = \eta\text{-}C_5Me_5$) affords $[MoCp^*Cl_4(Ph_2PCH_2C_3H_4NO\text{-}\kappa^1P)]$ as a kinetic isomer, which then transforms quantitatively to $[MoCp^*Cl_3(Ph_2PCH_2C_3H_4NO\text{-}\kappa^2P,N)]^+Cl^-$, **3**. Ligand **II** reacts with $[MoCp(\mu\text{-}Cl)_2]_2$ ($Cp = \eta\text{-}C_5H_5$) to afford the adduct $[CpMoCl_2\{Ph_2PCH_2C(O)NPh_2\text{-}\kappa^2P,O\}]$, **4**, as an equilibrium mixture of two isomers. Longer reaction times in CH_2Cl_2 lead to the molybdenum(IV) by-product $[MoCpCl_3\{Ph_2PCH_2C(O)NPh_2\text{-}\kappa^2P,O\}]$, **5**. While ligand **II** does not react with $[MoCp^*(\mu\text{-}Cl)_2]_2$, it does so in the presence of 1 equivalent of $AgBF_4$ to afford $[MoCp^*Cl_2\{Ph_2PCH_2C(O)NPh_2\text{-}\kappa^2P,O\}][BF_4]$, **6**. Further reaction with CH_2Cl_2 leads to $[MoCp^*Cl_3\{Ph_2PCH_2C(O)NPh_2\text{-}\kappa^2P,O\}]$ $[BF_4]$, **7**. The direct reaction between $[MoCp^*Cl_4]$ and ligand **II** affords $[MoCp^*Cl_4\{Ph_2PCH_2C(O)NPh_2\text{-}\kappa^1P\}]$ **8** as a kinetic isomer which then slowly establishes a solvent-dependent equilibrium with the ionic isomer $[MoCp^*Cl_3\{Ph_2PCH_2C(O)NPh_2\text{-}\kappa^2P,O\}]^+ Cl^-$. The solid state structure of compounds **5** and **7** has been determined by single crystal X-ray diffraction. The chemical, spectroscopic, and electrochemical data indicate that ligand **II** has a greater hemilabile character than ligand **I**.

Introduction

Molybdenum(III) half-sandwich complexes are known as mononuclear $[MoCpX_2L_2]$, $[MoCpXL_3]^+$ and $[MoCpL_4]^{2+}$ and as dinuclear $[Mo_2Cp_2X_4(\mu\text{-}X)]^-$, $[MoCp(\mu\text{-}X)_2]_2$, $[Mo_2Cp_2L_2(\mu\text{-}X)_3]^+$ and $[\{MoCpL_2(\mu\text{-}X)\}_2]^{2+}$ and have shown compatibility with a large array of ligands. Examples with X = halide,[1–5] hydrosulfido, alkane- and aryenethiolato,[6–9] amido,[10] dialkylphosphido,[11] phenyldiazo,[12] isocyanato,[13] azido,[14] alkyl,[15] and hydroborate units,[16] L = phosphine,[17–21] CO[22–26] isocyanides[27,28] and MeCN,[27,29,30] L_2 = diphosphines,[31–33] phosphine sulfides[34] and dienes,[35–38] and XL = phosphine–thiolato[34] and allyl[37–40] have been reported. Our own work in this area has been summarized in review articles.[41–44] Interest in these compounds ranges from modelling the activity of nitrogenase enzymes and hydrodesulfurization catalysts to the quest for new polymerization catalysts. The possibility to link bifunctional ligands having a soft and a hard donor atom may open new opportunities in terms of chemical reactivity and catalysis by virtue of the hemilability concept and in terms of establishing new building blocks for the assembly of heterobimetallic architectures.[45,46] We have extended the chemistry of this class of compounds to the bifunctional ligands 2-(diphenylphosphinomethyl)oxazoline **I** and diphenylphosphino-*N*,*N*-diphenylacetamide **II**, and report here our results, which also involve the generation of a few related species in the oxidation states IV and V. The complexes obtained are the first examples of this class where co-ordination by O- and N-based (except for the above mentioned MeCN complexes) L ligands is demonstrated.

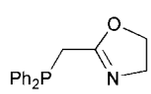

I

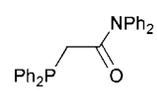

II

Experimental

General

All reactions involving air- and moisture-sensitive organometallic compounds were carried out in a Jacomex glove-box or by the use of standard Schlenk techniques under an argon atmosphere. The solvents were dried by conventional methods (THF, toluene and pentane from sodium–benzophenone and CH_2Cl_2 from P_4O_{10}) and distilled under argon prior to use. ^1H NMR measurements were carried out on a Bruker AC200 spectrometer. The peak positions are reported with positive shifts in ppm downfield of TMS as calculated from the residual solvent peaks. The IR spectra were recorded on a Bruker IFS 66V spectrophotometer with NaCl optics. EPR measurements were carried out at the X-band microwave frequency on a Bruker ESP300 spectrometer. The spectrometer frequency was calibrated with diphenylpicrylhydrazyl (DPPH, $g = 2.0037$). Cyclic voltamograms were recorded with an EG&G 362 potentiostat connected to a Macintosh computer through MacLab hardware/software. The electrochemical cell was fitted with a Ag–AgCl reference electrode, a platinum disk working electrode and a platinum wire counterelectrode. $[Bu_4N]PF_6$ (*ca.* 0.1 M) was used as supporting electrolyte. All potentials are reported relative to the ferrocene standard, which was added to

DOI: 10.1039/b002403l

This journal is © The Royal Society of Chemistry 2000

each solution and measured at the end of the experiments. The magnetic susceptibility measurements were carried out at room temperature with a Johnson Matthey magnetic balance which operates with a modified Gouy method, whereby the effect of the sample on the weight of the magnet, rather than the effect of the magnet on the weight of the sample, is used to retrieve the susceptibility information. The elemental analyses were carried out by the analytical service of the Laboratoire de Synthèse et d'Electrosynthèse Organométallique with a Fisons EA 1108 apparatus. Compounds [MoCp*Cl_4],[47] [MoCp*(μ-Cl)$_2$]$_2$,[48] [MoCp(μ-Cl)$_2$]$_2$,[49,50] and the ligands 2-(diphenylphosphinomethyl)oxazoline[45] and diphenylphosphino-*N*,*N*-diphenylacetamide[51] were prepared as described in the literature.

Preparations

[MoCpCl_2(Ph$_2$P$CH_2$$C_3H_4$NO)], 1. A solution of ligand **I** (0.160 g, 0.59 mmol) in 5 mL of CH_2Cl_2 was added to a suspension of [MoCp(μ-Cl)$_2$]$_2$ (0.137 g, 0.29 mmol) in 10 mL of CH_2Cl_2 at room temperature. The insoluble starting material disappeared after stirring for 30 min and the resulting brown solution was filtered through Celite. Addition of 20 mL of pentane gave complex **1** as a microcrystalline grey solid, which was filtered off, washed with pentane (3 × 5 mL) and dried *in vacuo*. Yield: 0.112 g, 38%. Calc. for $C_{21}H_{21}Cl_2MoNOP$: C, 50.32; H, 4.22; N, 2.79. Found: C, 50.44; H, 4.28; N, 2.63%. IR (Nujol mull): 1617 cm^{-1}. EPR (CH_2Cl_2): $g = 1.972$ (d with molybdenum satellites, $a_{Mo} = 40.2$, $a_P = 21.3$ G). Cyclic voltammetry (CH_2Cl_2): reversible oxidation at $E_{1/2} = 0.17$ V. Compound **1** is insoluble in all common hydrocarbon solvents and only slightly soluble in THF. After isolation as a solid from CH_2Cl_2 solution, it also exhibited sparing solubility in this solvent. It is quite air sensitive, becoming immediately brown upon exposure to air.

Carrying out the reaction between [MoCp(μ-Cl)$_2$]$_2$ (0.370 g, 0.80 mmol) and ligand **I** (0.370 g, 1.59 mmol) in THF as solvent (20 mL), led to the precipitation of compound **1** from the reaction mixture. Yield: 0.492 g, 61%. Dichloromethane solutions of this product exhibited an EPR spectrum identical to that of the product obtained directly from CH_2Cl_2.

[MoCp*Cl_2(Ph$_2$P$CH_2$$C_3H_4$NO)], 2. To a solution of [MoCp*(μ-Cl)$_2$]$_2$ (0.319 g, 0.52 mmol) in 10 mL of CH_2Cl_2 was added a solution of **I** (0.284 g, 1.059 mmol) in 5 mL of CH_2Cl_2 at room temperature, followed by stirring for 3 h. The resulting green-brown solution was evaporated to dryness, the solid extracted with warm toluene, and the solution was filtered through Celite and cooled to room temperature to give complex **2** as a microcrystalline green solid. The product was isolated by filtration, washed with pentane (3 × 5 mL) and dried *in vacuo*. Yield: 0.209 g, 35%. Calc. for $C_{26}H_{31}Cl_2MoNOP$: C, 54.66; H, 5.47; N, 2.45. Found: C, 54.44; H, 5.33; N, 2.78%. IR (Nujol mull): 1616 cm^{-1}. EPR (CH_2Cl_2): $g = 1.982$ (d, with molybdenum satellites, $a_{Mo} = 39.8$, $a_P = 19.3$ G). Cyclic voltammetry (CH_2Cl_2): reversible oxidation at $E_{1/2} = -0.74$ V (*vs* ferrocene).

[MoCp*Cl_4(Ph$_2$P$CH_2$$C_3H_4$NO)], 3. A solution of **I** (0.160 g, 0.59 mmol) in 5 mL of CH_2Cl_2 was added to a suspension of [MoCp*Cl_4] (0.223 g, 0.59 mmol) in 20 mL of CH_2Cl_2 at 0 °C. The solution was warmed to room temperature and an aliquot immediately withdrawn for an EPR investigation: doublet with molybdenum satellites, $g = 1.986$, $a_{Mo} = 44.2$, $a_P = 26.1$ G. The solution was stirred overnight and then filtered through Celite. The filtrate was concentrated under reduced pressure to *ca*. 1 mL. Addition of 20 mL of pentane gave complex **3** as a red microcrystalline solid, which was filtered off, washed with pentane (4 × 5 mL) and dried *in vacuo*. Yield: 0.220 g, 57%. Calc. for $C_{26}H_{31}Cl_4MoNOP$: C, 48.62; H, 4.86; N, 2.18. Found: C, 48.23; H, 4.80; N, 2.09%. EPR: (CH_2Cl_2) $g = 1.978$ (d, with molybdenum satellites, $a_{Mo} = 45.7$, $a_P = 25.5$ G); (THF or MeCN) $g = 1.962$ (broad d, $a_P = 27.4$ G). Cyclic voltammetry (CH_2Cl_2): reversible reduction at $E_{1/2} = -1.096$ V (*vs*. ferrocene). Compound **3** is insoluble in pentane and in Et_2O.

[MoCpCl_2{Ph$_2$PCH_2C(O)NPh_2-κ^2*P*,*O*}], 4. To a solution of **II** (0.418 g, 1.06 mmol) in 5 mL of CH_2Cl_2 was added a suspension of [MoCp(μ-Cl)$_2$]$_2$ (0.463 g, 1.00 mmol). After stirring for 1 h the resulting red brown solution was filtered through Celite. The filtrate was evaporated to dryness and the residue extracted with toluene (20 mL) and filtered. Addition of 2 × 10 mL of pentane gave complex **4** as a brick-red powder, which was filtered off, washed with pentane (2 × 10 mL) and dried *in vacuo*. Yield: 0.225 g, 32%. Calc. for $C_{31}H_{27}Cl_2MoNOP$: C, 59.35; H, 4.34; N, 2.23. Found: C, 58.89; H, 4.34; N, 2.27%. IR (CH_2Cl_2): ν(CO) 1554 cm^{-1}. EPR (CH_2Cl_2): overlap of two doublets with molybdenum satellites; 1st species (55.1%), $g = 1.977$, $a_P = 11.7$, $a_{Mo} = 38.7$ G; 2nd species (44.9%), $g = 1.971$, $a_P = 12.2$ G, $a_{Mo} = 37.8$ G. Cyclic voltammetry (CH_2Cl_2): reversible oxidation at $E_{1/2} = 0.43$ V. The voltammogram also showed a smaller reversible oxidation wave with $E_{1/2} = 0.19$ V, due to the by-product **5** (see below).

An analogous preparative procedure was carried out from **II** (0.590 g, 1.49 mmol) and [MoCp(μ-Cl)$_2$]$_2$ (0.346 g, 0.75 mmol) in 25 mL of CH_2Cl_2, a difference being that the mixture was stirred overnight. After filtration through Celite, the filtrate was evaporated to dryness and the residue extracted with hot toluene (30 mL) and filtered. The precipitate which formed upon cooling was separated by decanting off the mother-liquor, dried and redissolved in CH_2Cl_2 (10 mL). Diffusion of a pentane layer (20 mL) afforded crystals of complex **5**·CH_2Cl_2 (*ca*. 0.030 g) over 1 week, one of which was used for the X-ray analysis. Calc. for $C_{32}H_{29}Cl_5MoNOP$: C, 51.40; H, 3.91; N, 1.87. Found: C, 51.17; H, 3.76; N, 2.09%. ^{1}H NMR ($CDCl_3$, 297 K): δ 7.6–7.2 (m, 20 H, Ph), 5.35 (br s, 5 H, $w_{1/2} = 50$, Cp), 5.28 (s, 2 H, CH_2Cl_2) and 4.21 (br s, 2 H, $w_{1/2} = 25$ Hz, CH_2). Upon warming, the Cp peak broadened and disappeared at 309 K, while the CH_2 peak shifted and broadened ($w_{1/2} = 40$ Hz) to δ 4.06. Upon cooling to 270 K, sharp Cp (s) and CH_2 (d, $J_{PH} = 9$ Hz) resonances were observed at δ 5.31 and 4.25, respectively. ^{31}P-{^{1}H} NMR ($CDCl_3$, 297 K): δ 57.1 ($w_{1/2} = 70$ Hz). Cyclic voltammetry (CH_2Cl_2): reversible oxidation at $E_{1/2} = 0.43$ V.

[MoCp*Cl_2{Ph$_2$PCH_2C(O)NPh_2-κ^2*P*,*O*}]BF_4, 6. A solution of **II** (0.327 g, 0.82 mmol) in 5 mL of CH_2Cl_2 was added to a solution of [MoCp*(μ-Cl)$_2$]$_2$ (0.250 g, 0.41 mmol) in 15 mL of CH_2Cl_2 at room temperature, followed by stirring for 3 h. NMR and EPR monitoring showed the absence of any interaction between the two reagents. The solution was then added to $AgBF_4$ (0.161 g, 0.82 mmol) resulting in an immediate color change and the precipitation of a dark solid. After 30 min of stirring at room temperature the resulting mixture was filtered through Celite and the red-brown filtrate evaporated to dryness. Extraction of the residue with warm toluene (20 mL), followed by filtration and cooling to room temperature, gave complex **6** as red crystals (yield 0.17 g, 26%). Calc. for $C_{36}H_{37}BCl_2F_4MoNOP$: C, 55.13; H, 4.75. Found: C, 55.19; H, 4.42%. IR (CH_2Cl_2): ν(CO) 1540; ν(BF_4) 1061 cm^{-1}. ^{1}H NMR ($CDCl_3$, 297 K): δ 16.0 (br s, $w_{1/2} = 70$, Ph), 12.3 (br s, $w_{1/2} = 130$, Ph), *ca*. 9.8 (sh, $w_{1/2} = 100$, Ph), 9.7 (br s, $w_{1/2} = 35$, Ph), 9.3 (br s, $w_{1/2} = 30$, Ph), 8.3–8.1 (br m, total $w_{1/2} = 75$, Ph), 7.4 (s, overlaps with solvent peak, Ph), 6.8 (br s, $w_{1/2} = 30$, Ph), 6.3 (br s, $w_{1/2} = 110$, Ph), 3.6 (br s, 15 H, $w_{1/2} = 290$, Cp*), −9.0 (br s, 1 H, $w_{1/2} = 300$, CH_2) and −65.8 (br s, 1 H, $w_{1/2} = 400$ Hz, CH_2).

Recrystallization of complex **6** (0.070 g) by diffusion of a toluene layer (25 mL) into a CH_2Cl_2 solution (10 mL) over 1 week afforded crystals of [MoCp*Cl_3{Ph$_2$PCH_2C(O)NPh_2-κ^2*P*,*O*}]BF_4, **7**, which were used for the X-ray analysis. EPR

(CH_2Cl_2): doublet with molybdenum satellites, $g = 1.979$, $a_{Mo} = 44.0$, $a_P = 25.2$ G.

[MoCp*Cl$_4${Ph$_2$PCH$_2$C(O)NPh$_2$}], 8. A solution of **II** (0.045 g, 0.11 mmol) in 5 mL of THF was added at room temperature to a suspension of MoCp*Cl$_4$ (0.043 g, 0.11 mmol) in 5 mL of THF. The solid immediately dissolved to yield an orange-brown solution. An EPR spectrum was recorded immediately, showing a main doublet with molybdenum satellites (g = 1.986, $a_{Mo} = 43.0$, $a_P = 26.7$ G) and a smaller doublet at $g = 1.976$, $a_P = 26.0$ Hz. The solution was stirred overnight and an EPR spectrum recorded again. The weaker doublet at $g = 1.976$ had increased (see Results section). The EPR properties of this solution did not further evolve upon more prolonged stirring. An IR spectrum of the equilibrium THF solution was also recorded (see Results section).

X-Ray analysis

Compound 5·CH$_2$Cl$_2$. A red crystal (0.20 × 0.16 × 0.12 mm) suitable for an X-ray analysis was obtained by layering n-pentane onto a saturated methylene chloride solution at room temperature. The crystal was mounted on an Enraf-Nonius KappaCCD diffractometer equipped with Mo-Kα radiation. Absorption corrections were applied to the data during integration by the SCALEPACK [52] algorithm. The structure was solved via a Patterson search program [53] and refined (space group $P\bar{1}$) with full-matrix least-squares methods [53] based on $|F^2|$. All non hydrogen atoms were refined with anisotropic thermal parameters. The hydrogen atoms of the complex were included in their calculated positions and refined with a riding model. Crystal data are collected in Table 1 and selected bond distances and angles are listed in Table 2.

Compound 7. A small brown crystal (0.22 × 0.10 × 0.05 mm) suitable for an X-ray analysis was obtained by layering toluene onto a saturated methylene chloride solution at room temperature. The crystal was mounted on an Enraf-Nonius KappaCCD using MoKα radiation. Although the final Fourier difference map exhibited strong electron density close to the molybdenum atom (1.98 and −1.02 e Å^{-3}), any tentative to apply absorption corrections failed to fix the problem, thus no correction was applied. The structure was solved and refined (space group $P2_1/n$) as above.

CCDC reference number 186/2025.

See http://www.rsc.org/suppdata/dt/b0/b002403l/ for crystallographic files in .cif format.

Results and discussion

(a) Phosphinomethyloxazoline complexes

Compounds **1** and **2** are obtained by addition of ligand **I** to the dinuclear complexes [Mo(η-C$_5$R$_5$)(μ-Cl)$_2$]$_2$ (R = H or Me) as shown in eqn. (1). The products have been characterized by C,H,N analysis, IR and EPR spectroscopic methods and cyclic voltammetry. All data are consistent with the mononuclear formulation shown with a chelating (P,N) ligand.

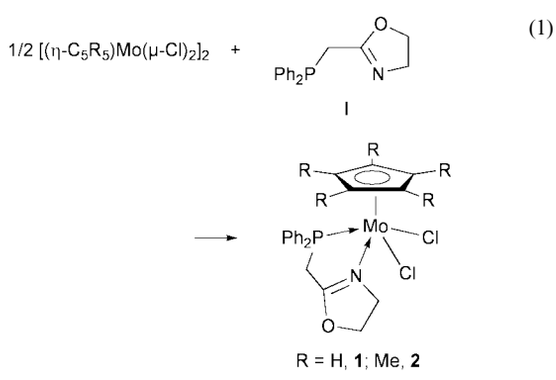

(1)

The IR spectrum shows strong C=N stretching vibrations for the oxazoline ring at 1617 and 1616 cm^{-1} for complexes **1** and **2**, respectively. These are 43–44 cm^{-1} red-shifted relative to the "free" ligand (1660 cm^{-1}). Other N-co-ordinated oxazoline complexes also display red-shifted absorptions, for instance from 1661 to 1648 and 1649 cm^{-1} upon co-ordination of the bis(oxazolinyl)phosphine ligand PhP(CH$_2$C$_3$H$_4$NO-2)$_2$ to ruthenium(II) centres.[54] Oxygen co-ordination (to our knowledge yet unreported), on the other hand, would be expected to result in a smaller or even opposite shift of the C=N absorption. The IR evidence, therefore, agrees with N-co-ordination for the phosphinomethyloxazoline ligand.

The X-band EPR spectrum for each compound shows a distinctive central doublet resonance ($g = 1.972$ for **1**, 1.982 for **2**) showing coupling to a single phosphorus atom ($a_P = 21.3$ G for **1**, 19.3 G for **2**) flanked with satellites generated by the $I = 5/2$ molybdenum isotopes (25% abundance; $a_{Mo} = 40.2$ G for **1**, 39.8 G for **2**). The EPR spectra therefore establish phosphorus co-ordination for the ligand. The similarity of the coupling constants indicates that the two compounds adopt the same stereochemistry. It was previously reported for analogous Ph$_2$PCH$_2$CH$_2$PPh$_2$ (dppe) derivatives that a relative *cis* configuration in complexes [MoCpX$_2$(dppe)] (as verified by X-ray crystallography for X = Br) [32] gave a_P hyperfine constants in the 18–26 G range (26 G for the dichloride), while the structurally characterized *trans* dichloride derivatives [MoCpCl$_2$(PR$_3$)$_2$] (PR$_3$ = PMe$_3$, PMePh$_2$, PPh$_3$ or PEt$_3$) [19,20,55] have a_P in the 9–16 G range [20] and complex [Mo{η-C$_5$H$_3$-(SiMe$_2$CH$_2$PPr$^i_2$-1,3)$_2$}-Cl$_2$], also showing a *trans* relative arrangement in the solid state, has $a_P = 15.2$ G.[21] For these reasons, we prefer to assign a *cis* relative arrangement to both compounds **1** and **2**, although an unambiguous assignment can only be provided by a single crystal X-ray study. Unfortunately, suitable crystals for such a determination could not be obtained for either compound.

The cyclic voltammograms of compounds **1** and **2** show a reversible oxidation wave at 0.17 and −0.74 V *vs.* ferrocene, respectively. All compounds of the type [MoCpX$_2$L$_2$] show a one-electron oxidation process of which the potential and reversibility depend on the nature of X and L. For instance, a reversible process is observed in the −0.4 to −0.6 V range for [MoCpCl$_2$(PR$_3$)$_2$] [41] and at −0.33 V for [MoCpCl$_2$(dppe)], [32] while the same process is shifted to −1.1 V for [MoCpCl$_2$-(η^4-C$_4$H$_6$)] [35] and to 0.12 V for [MoCpCl$_2$(Ph$_2$PCH$_2$CH$_2$SMe)]. [34] Therefore, according to the cyclic voltammetric data, the relative ability of the N-co-ordinated oxazoline moiety in the chelate to stabilize the molybdenum(III) and -(IV) species involved in the oxidation process is similar to that of the S-co-ordinated −CH$_2$SMe moiety. The negative shift observed on going from Cp to Cp* is consistent with the greater electron donating power of the latter. The magnitude of this shift (0.91 V), however, is quite large when compared to other Cp and Cp* bis(phosphine) complexes [0.32 V for [Mo(η-C$_5$R$_5$)Cl$_2$(PMe$_3$)$_2$] and 0.25 V for [Mo(η-C$_5$R$_5$)Cl$_2$(dppe)] on going from R = H to Me]. [26,56] A possible rationalization of this effect is to invoke a greater ability of the π-acidic phosphorus donors to buffer the electron density variations caused by the different cyclopentadienyl substitution.

In an attempt to find a more convenient synthetic method for compound **2**, ligand **I** was added to [MoCp*Cl$_4$], yielding the corresponding adduct **3**, eqn. (2). Monitoring this reaction by EPR spectroscopy (Fig. 1) revealed the immediate formation of an intermediate, followed by the slow rearrangement (12 h) to the isolated product. Both compounds show similar hyperfine splittings for Mo and P. It seems reasonable to propose that the compound which forms immediately corresponds to an adduct with the P-co-ordinated monodentate ligand, **A**, with a structure related to those determined for [M(η-C$_5$R$_5$)Cl$_4$(PR$_3$)] (M = Mo or W), namely with the phosphine ligand located

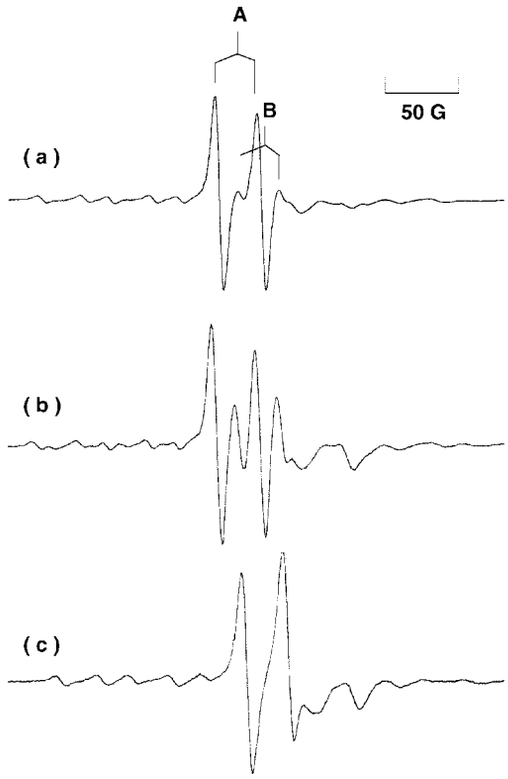

Fig. 1 EPR monitoring of the room temperature reaction between [MoCp*Cl$_4$4] and ligand **I** in CH_2Cl_2. (a) After 15 minutes; (b) after 1.5 h; (c) after 12 h.

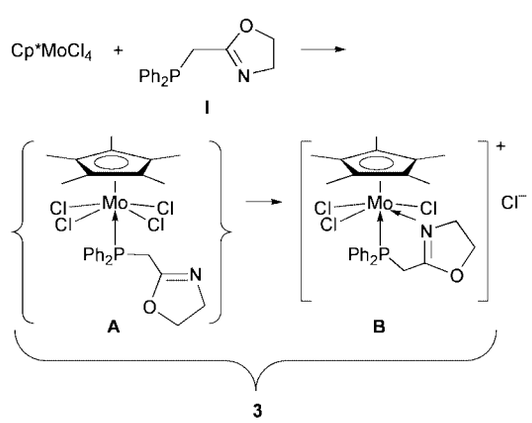

(2)

trans relative to the Cp* ligand.[57,58] The final product, on the other hand, probably involves chelation of the ligand with displacement of a chloride ligand from the co-ordination sphere, as indicated in **B**. The structure of the cation would be identical to that determined for the cation of compound **7** containing ligand **II**, see below, whose EPR parameters are essentially identical to those of **B** and significantly different from those of the reaction intermediate **A**. Another related structure is that of [MoCp*Cl$_3${S$_2$P(OEt)$_2$}],[59] where the bidentate dithiophosphate ligand occupies the axial and one of the equatorial positions. The reduction of compound **3** (thermodynamic isomer **B**) with two equivalents of sodium failed to yield **2** and the characterization of the reduction product was therefore not pursued.

(b) Phosphine amide complexes

The addition reactions of the phosphine amide ligand **II** are more complex than those of ligand **I**. With [MoCp(μ-Cl)$_2$]$_2$ the reaction leads to the formation of the desired ligand adduct [MoCpCl$_2${Ph$_2$PCH$_2$C(O)NPh$_2$-κ^2*P*,*O*}], **4**, which is however accompanied by the formation of a molybdenum(IV)

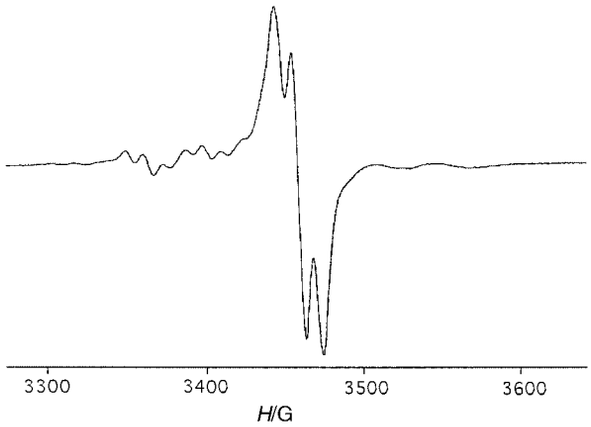

Fig. 2 Room temperature X-band EPR spectrum of compound **4** in CH_2Cl_2 solution.

by-product. The latter corresponds to the neutral trichloride derivative [MoCpCl$_3${Ph$_2$PCH$_2$C(O)NPh$_2$}], **5** (see below). The formation of this by-product is more pronounced when the reaction time in CH_2Cl_2 is longer, in agreement with a slow Cl atom abstraction from the solvent by the first reaction product **4**. When the reaction was stopped soon after the complete comsumption of the [MoCp(μ-Cl)$_2$]$_2$ starting material (1 h) elemental analysis and cyclic voltammetry (see below) of the isolated product indicated only a minor contamination by **5**. Compound **4** was also obtained by carrying out the reaction in THF, as confirmed by EPR spectroscopy and cyclic voltammetry, but the analytical purity of this sample was not superior to that of the reaction product from CH_2Cl_2.

An additional complication is that the EPR spectrum of the molybdenum(III) product **4** appears as a distorted triplet (Fig. 2). However, this is interpreted as the overlap of two doublets that are assigned to two different isomers of the adduct [MoCpCl$_2${Ph$_2$PCH$_2$C(O)NPh$_2$-κ^2*P*,*O*}], **4** (see eqn. 3). Both materials obtained from CH_2Cl_2 or THF show identical EPR properties. Variable temperature EPR measurements did not improve the resolution. However, a satisfactory digital fitting of the spectrum confirms the co-ordination of just one P donor atom for both isomers and provides the spectral parameters as well as the relative proportion of the two species.

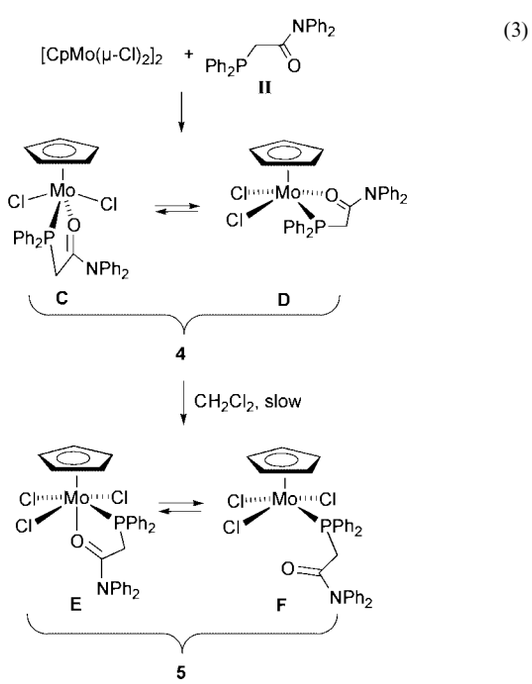

(3)

The IR spectrum contains a single and strong ν(C=O) band at 1554 cm^{-1}, showing that both isomers have a similar environment for the amide function. The "free" ligand[51] exhibits this absorption at 1658 cm^{-1}, while previously described co-ordination compounds with analogous phosphine amide ligands display absorptions around 1650 cm^{-1} when N-co-ordinated [*e.g.* for $(Ph_2P)_2CHC(O)NPh_2$][60] and around 1560 cm^{-1} when O-co-ordinated.[51] Thus, the IR results document O-co-ordination for the ligand in both isomers of compound **4**. Given that both species appear to contain the phosphine amide ligand in the same co-ordination mode (κ^2P,O), we propose that these are stereoisomers differing by the relative configuration at the metal center. Since both cisoid and transoid arrangements of 4-atom chelating ligands have been reported for $[Mo(\eta\text{-}C_5R_5)X_2L_2]$ complexes, for instance cisoid for $[MoCpBr_2(dppe)]$[32] and transoid for the more sterically encumbered $[MoCp^*Cl_2(dppe)]$,[61] it seems reasonable to propose that these two alternative arrangements, shown as **C** and **D** in eqn. (3), are responsible for the isomerism of **4**. The bulkier nature of ligand **II** would presumably force the structure to access the sterically less congested, but orbitally disfavored, transoid structure.

The cyclic voltammogram of compound **4** shows only one oxidation wave at $E_{1/2} = 0.43$ V. This observation indicates that the rate of interconversion of the two isomers of **4** is fast on the cyclic voltammetric timescale, while it is slow on the EPR timescale. The same phenomenon has been observed for other $MoCp^{III}$ derivatives.[20] The $E_{1/2}$ value is slightly higher than that of compound **1**, suggesting that the amide function in **II** is a poorer donor than the oxazoline function in **I**.

As stated above, the molybdenum(IV) by-product **5** was also obtained, in addition to **4**, when ligand **II** was treated with $[MoCp(\mu\text{-}Cl)_2]_2$ in CH_2Cl_2 and crystallized selectively after long contact times in this solvent. Compound **5** has been characterized by ^{1}H NMR spectroscopy, cyclic voltammetry, elemental analysis (C, H, N), and by X-ray crystallography (see below). The cyclic voltammogram shows a reversible oxidation wave at $E_{1/2} = 0.19$ V, *i.e.* 0.24 V less positive than the oxidation of **4**. This signifies that donation from one additional Cl^- ligand more than compensates for the electron density loss associated to the one-electron oxidation. This situation is analogous to that of the corresponding $[MoCpCl_n(dppe)]$ complexes ($E_{1/2} = -0.33$ V for $n = 2$ and -0.39 for the ax-eq isomer, *i.e.* isostructural with **5**, with $n = 3$).[26] The ^{1}H NMR spectrum of **5** is consistent with a ground state diamagnetism, in agreement with its 18-electron configuration, but shows abnormally broad resonances for the Cp and methylene protons. The ^{31}P NMR resonance is also abnormally broad. A variable temperature study shows that these resonances sharpen and shift slightly upon cooling, consistent with a thermal equilibrium between the diamagnetic ground state and a higher energy paramagnetic species. This behaviour is not consistent with a fast equilibration between two diamagnetic species, because in that case the resonances would sharpen upon warming in the fast exchange limit (only one set of resonances), contrary to the observation. Previous studies have shown that 16-electron derivatives of formula $[MoCpCl_2L_2]^+$ and $[MoCp^*Cl_3L]$ (L = tertiary phosphine) adopt a spin triplet ground state. Therefore, we propose that the NMR properties result from a thermal equilibrium between the diamagnetic 18-electron structure observed in the solid state, **E**, and a paramagnetic 16-electron structure resulting from deco-ordination of the amide function, **F** [eqn. (3)].

Complex $[MoCp^*(\mu\text{-}Cl)_2]_2$ does not show any reactivity with ligand **II**. This contrasts with both the reactivity of the Cp analogue with the same ligand and with that of the same MoCp* complex with ligand **I** (see above). However, when one equivalent of Ag^+ per Mo atom is added as the BF_4^- salt to a CH_2Cl_2 solution containing $[MoCp^*(\mu\text{-}Cl)_2]_2$ and ligand **II** a redox process takes place and complex $[MoCp^*Cl_2\{Ph_2PCH_2C(O)NPh_2\text{-}\kappa^2P,O\}]BF_4$, **6**, may be recovered from the solution, eqn. (4).

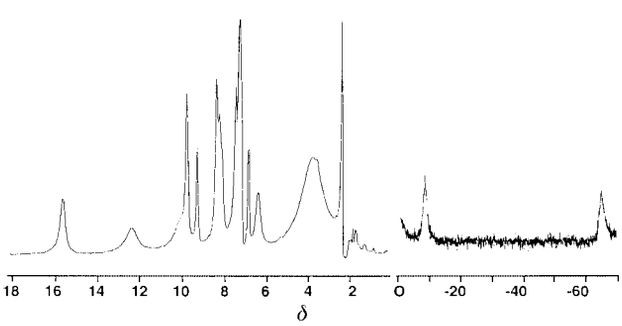

Fig. 3 Room temperature ^{1}H NMR spectrum of compound **6** in $CDCl_3$ solution.

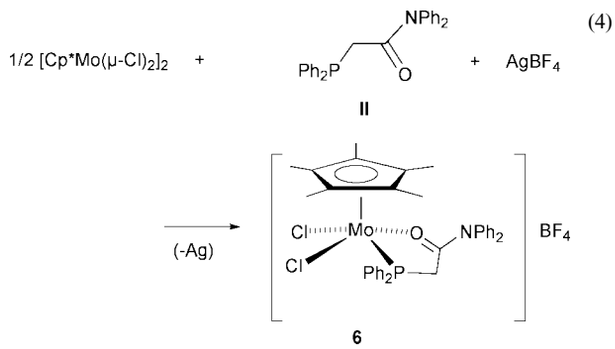

(4)

Complex **6** has been characterized by elemental analysis and by IR and ^{1}H NMR spectroscopy. The IR spectrum shows evidence for O-co-ordination, with a ν(CO) band at 1540 cm^{-1}. The ^{1}H NMR spectrum (see Fig. 3) indicates paramagnetism. Related spin triplet 16-electron half-sandwich molybdenum(IV) complexes, *e.g.* $[MoCpCl_2(PMe_3)_2]^+$ and $[MoCp^*Cl_3(PMe_3)]$,[19,62] exhibit similar shifts for the ^{1}H NMR resonances. On the basis of these precedents, we are able to assign the upfield shifts at δ -9.0 and -65.8 to the two inequivalent methylene protons and the strong resonance at δ 3.6 to the Cp* protons, while the 4 inequivalent phenyl groups yield 12 signals (11 of which are distinctly observed) that are all more or less shifted downfield by the electron spin density.

Attempts to grow single crystals of compound **6** from CH_2Cl_2–toluene afforded instead crystals of the related oxidized trichloride species, $[MoCp^*Cl_3\{Ph_2PCH_2C(O)NPh_2\text{-}\kappa^2P,O\}]BF_4$, **7**, which is characterized by an EPR spectrum essentially identical with that of the final product of reaction (2), *i.e.* **B**. The cation of compound **7** has also been generated by direct interaction between $[MoCp^*Cl_4]$ and ligand **II**, eqn. (5). EPR spectroscopy (Fig. 4) shows that the reaction

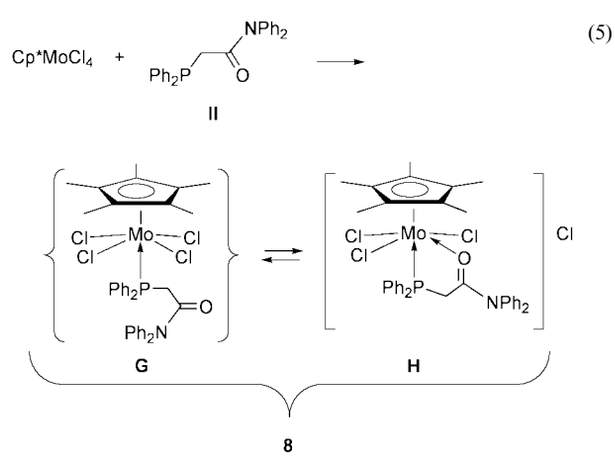

(5)

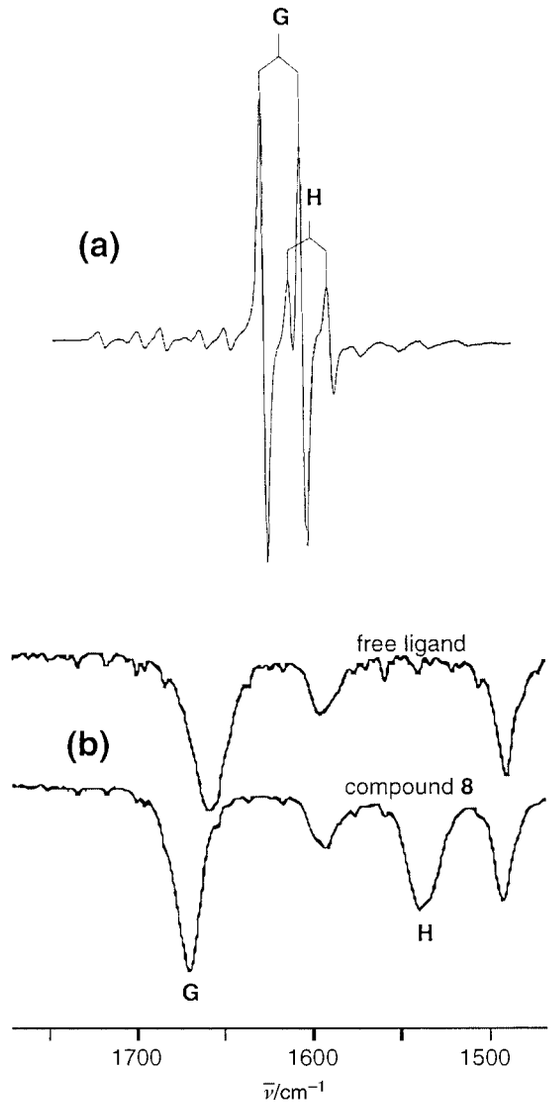

Fig. 4 Equilibrium spectral properties of compound **8** in THF solution at room temperature: (a) EPR spectrum; (b) IR spectrum in comparison with that of the "free" ligand.

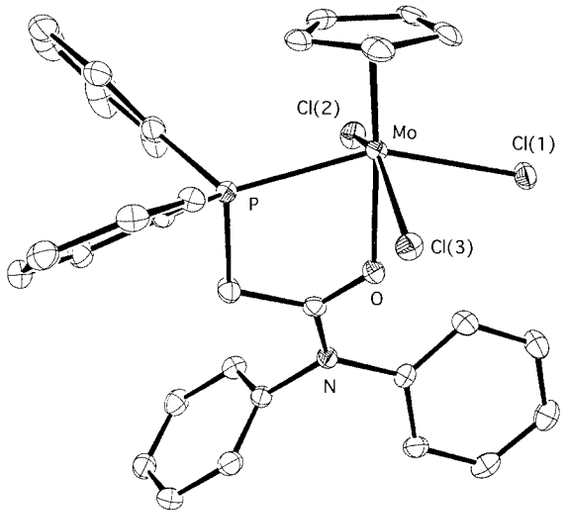

Fig. 5 An ORTEP[63] view of a molecule of complex **5**. Ellipsoids are shown at the 50% probability level.

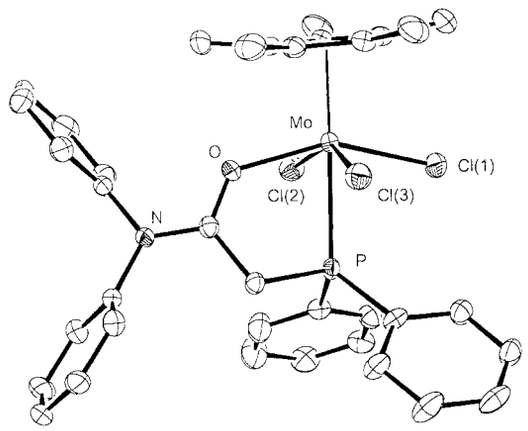

Fig. 6 An ORTEP view of the cation of complex **7**. Details as in Fig. 5.

follows a similar course to the corresponding reaction of [MoCp*Cl_4] with ligand **I**, namely a molecular adduct **G** is formed as immediate, followed by a structural rearrangement to the ionic isomer **H**. The EPR parameters of the kinetic product **G** are essentially identical with those of **A**, while those of **H** are essentially identical with those of **B** and superimposable with those of **7**. However, while the transformation of **A** to **B** [eqn. (2)] is quantitative, both the molecular and ionic isomers persist for compound **8**, the neutral isomer remaining the predominant species at equilibrium. This is in agreement with a weaker chelating power of ligand **II** relative to ligand **I**.

The presence of an isomeric equilibrium between monodentate and chelating forms is further supported by solution IR studies. A THF solution of complex **8** shows a major absorption at 1670 cm^{-1} for the unco-ordinated amide function of **G** (*cf.* 1658 cm^{-1} for the "free" ligand) and a smaller absorption at 1540 cm^{-1} for the O-co-ordinated amide function of **H** (see Fig. 4).

(c) Crystal structures

The geometries of compound **5** and of the cation of **7** are shown in Figs. 5 and 6, respectively, and the relevant bond distances and angles are compared in Table 2. As is immediately evident from the figures, both complexes adopt the same basic pseudo-octahedral geometry when considering the cyclopentadienyl ring as occupying a single co-ordination position. The three chloride ligands occupy three equatorial positions in both structures and the amide function is co-ordinated *via* the oxygen atom in both cases, confirming the indications obtained by IR spectroscopy. On the other hand, the orientation of the phosphine amide ligand is inverted in the two structures. For **5** the phosphorus atom occupies an equatorial position and the oxygen is in the axial position, while the reverse holds true for **7**. The reason for this change may have a steric origin. For the more sterically encumbered **7** the bulkier PPh_2 end of the chelating ligand is located farther from the bulky Cp* ligand. The less sterically congested **5**, however, may have an electronic preference for the observed structure. An analysis of the previously reported pseudo-octahedral [$MoCpCl_3L_2$] (L_2 = dppe or dmpe) complexes[64,65] shows that the axially co-ordinated P donor atom is less tightly bonded than the corresponding equatorial P atom, a situation that may be associated with the *trans* influence of the cyclopentadienyl ligand. Thus, the more strongly co-ordinated phosphorus donor in ligand **II** should have a greater tendency to occupy an equatorial position, leaving the labile oxygen end of the ligand to provide a supporting stabilization by co-ordinatively saturating the axial position.

The shortening of the Mo–Cl distances on going from complex **5** to **7** follows the expected decrease of the metal ionic radius upon increasing the oxidation state. The corresponding lengthening of the Mo-P distance, on the other hand, is related to the structural change which places the phosphorus

Table 1 Crystal data and structure refinement parameters for compounds **5**·CH_2Cl_2 and **7**

	5·CH_2Cl_2	**7**
Formula	$C_{31}H_{27}Cl_3MoNOP\cdot CH_2Cl_2$	$C_{36}H_{37}Cl_3MoNOP\cdot BF_4$
M	747.72	819.74
T/K	110(2)	110(2)
Crystal system	Triclinic	Monoclinic
Space group	$P\bar{1}$	$P2_1/n$
a/Å	11.1707(6)	12.354(1)
b/Å	11.8110(6)	14.895(1)
c/Å	12.2717(8)	19.937(1)
α/°	88.024(3)	
β/°	80.438(2)	106.961(2)
γ/°	79.718(3)	
V/Å^3	1570.9(2)	3509.1(4)
Z	2	4
μ/mm^{-1}	0.922	0.70
RC = Reflections collected	11333	24328
IRC = Independent RC	6814 [*R*(int) = 0.031]	8008 [*R*(int) = 0.08]
IRCGT = IRC and [$I > 2\sigma(I)$]	5916	5910
*R*1, *wR*2 for IRCGT	0.030, 0.065	0.064, 0.13
for IRC	0.039, 0.069	0.096, 0.15

Table 2 Selected bond distances (Å) and angles (°) for compounds **5**·CH_2Cl_2 and **7**[a]

	5·CH_2Cl_2	**7**
Mo–CNT	1.977(3)	2.082(5)
Mo–Cl(1)	2.4923(6)	2.3794(12)
Mo–Cl(2)	2.5309(6)	2.3888(13)
Mo–Cl(3)	2.4583(6)	2.3955(14)
Mo–P	2.4702(6)	2.6039(13)
Mo–O	2.143(2)	2.134(3)
C–O	1.255(3)	1.263(5)
C(O)–N	1.341(3)	1.331(6)
CNT–Mo–Cl(1)	106.2(1)	104.2(3)
CNT–Mo–Cl(2)	105.4(2)	105.3(3)
CNT–Mo–Cl(3)	105.4(2)	104.1(3)
CNT–Mo–P	101.9(2)	174.6(4)
CNT–Mo–O	176.6(4)	103.0(4)
Cl(1)–Mo–Cl(2)	85.90(2)	88.46(4)
Cl(1)–Mo–Cl(3)	84.32(2)	91.59(4)
Cl(1)–Mo–P	151.77(2)	78.89(4)
Cl(1)–Mo–O	77.08(4)	152.58(9)
Cl(2)–Mo–Cl(3)	149.11(2)	149.67(5)
Cl(2)–Mo–P	84.79(2)	79.12(4)
Cl(2)–Mo–O	74.38(4)	80.76(9)
Cl(3)–Mo–P	90.17(2)	71.15(4)
Cl(3)–Mo–O	74.89(4)	85.50(10)
P–Mo–O	74.76(4)	74.37(9)
C–C–O	119.1(2)	119.7(4)
C–C–N	119.8(2)	120.4(4)
O–C–N	121.0(2)	119.9(4)

[a] CNT = Cyclopentadienyl ring centroid.

donor in the more tightly bonded equatorial position in **5** and in the less tightly bonded axial position in **7**. Other related Mo–P distances are 2.542(1) and 2.553(1) Å (equatorial) for the molybdenum(IV) compound $[MoCpCl_3(PMe_2Ph)_2]$,[62] and 2.617(1) and 2.554(1) Å (axial) for the molybdenum(V) compounds $[Mo(C_5H_4Me)Cl_4(PH_2Ar)]$ (Ar = 2,4,6-$Pr^i_3C_6H_2$ or C_6H_5, respectively).[58] The Mo-O distance changes in the opposite direction, as expected.

(d) Comparison of the two ligands

Both ligands **I** and **II** contain, in addition to a Ph_2P donor group, a nitrogen and an oxygen-based donor function. However, **I** chose binds selectively with the nitrogen function, **II** with the oxygen function. This behaviour can easily be understood on the basis of the resonance forms shown in Scheme 1, where

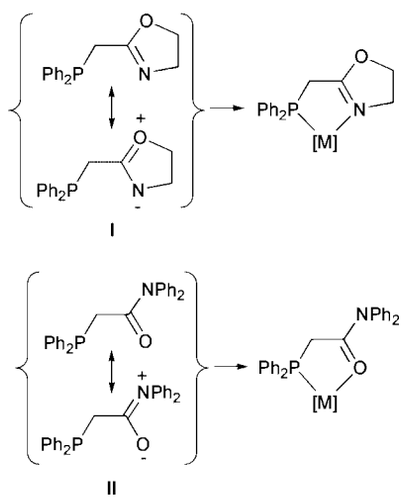

Scheme 1

an oxygen lone pair is seen to reinforce the donor power of the nitrogen function for **I** and the nitrogen lone pair reinforces the donor power of the oxygen function for **II**, as a result of a similar delocalization mechanism. Thus, in spite of a greater "oxophilicity" of molybdenum relative to the late transition metals, the phosphine oxazoline ligand **I** still binds preferencially with the nitrogen function and oxygen binding with this ligand remains undocumented.

While ligand **I** adds selectively to $[MoCp(\mu\text{-}Cl)_2]_2$ in CH_2Cl_2, **II** also provokes a chlorine abstraction process from the solvent. A similar chlorine abstraction was previously observed when treating $[MoCp^*Cl_2(PMe_2Ph)_2]$ with $AlCl_3$ in CH_2Cl_2.[66] It was proposed that the abstraction of a chloride ion by $AlCl_3$ produces the highly reactive 15-electron species $[MoCp^*Cl(PMe_2Ph)_2]^+$, which is capable of abstracting a Cl atom in order to produce the more stable 16-electron species $[MoCp^*Cl_2(PMe_2Ph)_2]^+$. A similar mechanism may therefore take place for the formation of compound **5** (Scheme 2). This observation may therefore be taken as an indication of a greater hemilabile character of ligand **II** relative to **I**. This is also demonstrated by the equilibrium between the κ^1P (major) and κ^2P,O (minor) forms of compound **8** (eqn. 5), while for ligand **I** the kinetically accessed κ^1P form of compound **3** transforms *quantitatively* to the κ^2P,N form (eqn. 2). However, the hemilability of ligand **II** in compound **8** is obviously related to the presence of the strongly co-ordinating Cl^- anion in the ionic form **H**. For the analogous salt **7** containing the less strongly co-ordinating

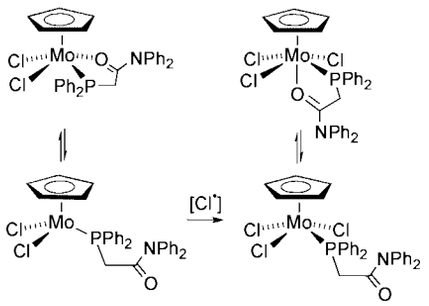

Scheme 2

BF_4^- anion the EPR properties indicate that only the κ^2P,O form is present in solution. The hemilabile properties of ligand **II** are also evidenced by a similar κ^1–κ^2 equilibrium for compound **5** (eqn. 3).

It has been argued in a previous section that the presence of two geometric isomers for compound **4**, while only one is observed for **1**, could arise from steric factors. On the same basis, one can rationalize the absence of an interaction between $[MoCp^*(\mu\text{-}Cl)_2]_2$ and ligand **II**. The addition of neutral ligands to dinuclear cyclopentadienyldichloromolybdenum(III) complexes is known to be delicately balanced from the thermodynamic point of view by steric effects.[66] As shown in Scheme 3,

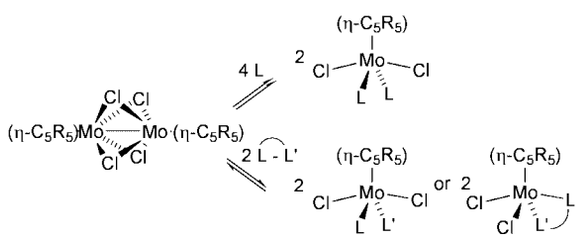

Scheme 3

the addition products have the same number of metal–ligand bonds as the reagent but four weaker Mo–Cl interactions are replaced by stronger Mo–L interactions. On the other hand, a metal–metal bond is lost. A quantitative reaction occurs for the Cp* precursor with L = PMe_3 or PMe_2Ph, whereas no reaction occurs with the bulkier ligands $PMePh_2$ and PPh_3,[66] while the analogous precursor with the sterically less demanding Cp ring reacts with all the above ligands.[20] The stability of a Cp* product with $Ph_2PCH_2CH_2PPh_2$, whose steric bulk is similar to that of two $PMePh_2$ ligands, illustrates how delicate this steric balance is.[61] Since ligand **II** should be less bulky than dppe, a weaker Mo–O=C(NPh_2) interaction relative to the Mo-PPh_2 interaction must also be invoked to rationalize the absence of an interaction between $[MoCp^*(\mu\text{-}Cl)_2]_2$ and ligand **II**.

The stability of the the cationic molybdenum(IV) and -(V) systems **6** and **7** demonstrates the steric compatibility of ligand **II** with the $[MoCp^*Cl_2]$ and even with the $[MoCp^*Cl_3]$ moiety, which is made even more stringent by the reduced size of Mo^{IV} and Mo^{V} relative to Mo^{III}. Consequently, the stability of the phosphine oxazoline Cp* complex **2** relative to the non-existent phosphine amide adduct may be attributed to the lower steric hindrance of the oxazoline ring, or to a greater strength for the Mo–oxazoline interaction, or to a combination of both factors.

Conclusion

The phosphine oxazoline and phosphine amide compounds **I** and **II** behave in similar but not identical ways as ligands toward half-sandwich complexes of Mo^{III}, Mo^{IV} and Mo^{V}. The observed differences can be traced to differences in steric and electronic properties: the weaker donor ability and greater bulk of the O-donating amide function relative to the N-donating oxazoline function make the former a less tightly bonded bidentate ligand. The greater hemilability exhibited by the phosphine amide ligand **II** is the source of greater reactivity. Therefore, the molybdenum complexes with the phosphine amide ligand **II** have greater potential for use as building blocks for the construction of more complex architectures and for catalytic applications.

Acknowledgements

We are grateful to the Ministère de l'Education Nationale, de la Recherche et de la Technologie (MENRT) for support and a PhD grant (to J.-M. C. and F. N.), the Centre National de la Recherche Scientifique and the Conseil Régional de Bourgogne for support of this work.

References

1 M. L. H. Green and P. Mountford, *Chem. Soc. Rev.*, 1992, 29, and references therein.
2 J. H. Shin and G. Parkin, *Polyhedron*, 1994, **13**, 1489.
3 R. Poli and A. L. Rheingold, *J. Chem. Soc.*, *Chem. Commun.*, 1990, 552.
4 J. U. Desai, J. C. Gordon, H.-B. Kraatz, V. T. Lee, B. E. Owens-Waltermire, R. Poli, A. L. Rheingold and C. B. White, *Inorg. Chem.*, 1994, **33**, 3752.
5 F. J. de la Mata, P. Giner and P. Royo, *J. Organomet. Chem.*, 1999, **572**, 155.
6 N. G. Connelly and L. F. Dahl, *J. Am. Chem. Soc.*, 1970, **92**, 7470.
7 M. Rakowski DuBois, *Chem. Rev.*, 1989, **89**, 1, and references therein.
8 M. Rakowski DuBois, *Polyhedron*, 1997, **16**, 3089, and references therein.
9 F. Y. Pétillon, P. Schollhammer, J. Talarmin and K. W. Muir, *Coord. Chem. Rev.*, 1998, **178–179**, 203, and references therein.
10 P. Schollhammer, F. Y. Pétillon, S. Poder-Guillou, J. Y. Saillard, J. Talarmin and K. W. Muir, *Chem. Commun.*, 1996, 2633.
11 K. Fromm and E. Hey-Hawkins, *Z. Anorg. Allg. Chem.*, 1993, **619**, 261.
12 P. Schollhammer, E. Guénin, F. Y. Pétillon, J. Talarmin, K. W. Muir and D. S. Yufit, *Organometallics*, 1998, **17**, 1922.
13 P. Schollhammer, S. Poder-Guillou, F. Y. Pétillon and J. Talarmin, *Inorg. Chim. Acta*, 1997, **261**, 117.
14 P. Schollhammer, F. Y. Pétillon, J. Talarmin and K. W. Muir, *J. Organomet. Chem.*, 1998, **560**, 245.
15 E. Le Grognec, R. Poli and L.-S. Wang, *Inorg. Chem. Commun.*, 1999, **2**, 95.
16 T. P. Fehlner, *J. Chem. Soc.*, *Dalton Trans.*, 1998, 1525, and references therein.
17 P. D. Grebenik, M. L. H. Green, A. Izquierdo, V. S. B. Mtetwa and K. Prout, *J. Chem. Soc.*, *Dalton Trans.*, 1987, 9.
18 R. T. Baker, J. R. Morton, K. F. Preston, A. J. Williams and Y. Le Page, *Inorg. Chem.*, 1991, **30**, 113.
19 S. T. Krueger, R. Poli, A. L. Rheingold and D. L. Staley, *Inorg. Chem.*, 1989, **28**, 4599.
20 R. Poli, B. E. Owens, S. T. Krueger and A. L. Rheingold, *Polyhedron*, 1992, **11**, 2301.
21 M. D. Fryzuk, L. Jafarpour and S. J. Rettig, *Organometallics*, 1999, **18**, 4050.
22 M. B. Gomes de Lima, J. E. Guerchais, R. Mercier and F. Y. Pétillon, *Organometallics*, 1986, **5**, 1952.
23 J. Courtot-Coupez, M. Guéguen, J. E. Guerchais, F. Y. Pétillon, J. Talarmin and R. Mercier, *J. Organomet. Chem.*, 1986, **312**, 81.
24 P. Schollhammer, F. Y. Pétillon, R. Pichon, S. Poder-Guillou, J. Talarmin, K. W. Muir and L. Manojlovic-Muir, *Organometallics*, 1995, **14**, 2277.
25 D. S. Tucker, S. Dietz, K. G. Parker, V. Carperos, J. Gabay, B. Noll, M. Rakowski Dubois and C. F. Campana, *Organometallics*, 1995, **14**, 4325.
26 J. C. Fettinger, D. W. Keogh and R. Poli, *J. Am. Chem. Soc.*, 1996, **118**, 3617.
27 M. Guéguen, F. Y. Pétillon and J. Talarmin, *Organometallics*, 1989, **8**, 148.
28 F. Barrière, Y. Le Mest, F. Y. Pétillon, S. Poder-Guillon, P. Schollhammer and J. Talarmin, *J. Chem. Soc.*, *Dalton Trans.*, 1996, 3967.
29 M. El Khalifa, M. Guéguen, R. Mercier, F. Y. Pétillon, J.-Y. Saillard and J. Talarmin, *Organometallics*, 1989, **8**, 140.

30 P. Schollhammer, F. Y. Pétillon, J. Talarmin and K. W. Muir, *Inorg. Chim. Acta*, 1999, **284**, 107.
31 M. L. H. Green, J. Knight and J. A. Segal, *J. Chem. Soc.*, *Dalton Trans.*, 1977, 2189.
32 S. T. Krueger, B. E. Owens and R. Poli, *Inorg. Chem.*, 1990, **29**, 2001.
33 C. Elschenbroich, T. Isenburg and A. Behrendt, *Inorg. Chem.*, 1995, **34**, 6565.
34 D. Morales, R. Poli, P. Richard, J. Andrieu and E. Collange, *J. Chem. Soc.*, *Dalton Trans.*, 1999, 867.
35 J. L. Davidson, K. Davidson, W. E. Lindsell, N. W. Murrall and A. J. Welch, *J. Chem. Soc.*, *Dalton Trans.*, 1986, 1677.
36 J.-F. Capon, P. Schollhammer, F. Y. Pétillon, J. Talarmin and K. W. Muir, *Organometallics*, 1999, **18**, 2055.
37 L.-S. Wang, J. C. Fettinger and R. Poli, *J. Am. Chem. Soc.*, 1997, **119**, 4453.
38 R. Poli and L.-S. Wang, *Polyhedron*, 1998, **17**, 3689.
39 O. Andell, R. Goddard, S. Holle, P. W. Jolly, C. Krüger and Y. H. Tsay, *Polyhedron*, 1989, **8**, 203.
40 P. W. Jolly, C. Krüger, C. C. Romão and M. J. Romão, *Organometallics*, 1984, **3**, 936.
41 R. Poli, *J. Coord. Chem. B*, 1993, **29**, 121.
42 R. Poli, *Acc. Chem. Res.*, 1997, **30**, 494.
43 R. Poli and L.-S. Wang, *Coord. Chem. Rev.*, 1998, **178–179**, 169.
44 R. Poli, *Synlett.*, 1999, 1019.
45 P. Braunstein, M. D. Fryzuk, M. Le Dall, F. Naud, S. J. Rettig and F. Speisen, *J. Chem. Soc.*, *Dalton Trans.*, 2000, 1067.
46 J. Andrieu, P. Braunstein, F. Naud and R. D. Adams, *J. Organomet. Chem.*, 2000, **601**, 43.
47 D. W. Keogh and R. Poli, in *Synthetic Methods of Organometallic and Inorganic Chemistry* (*Herrmann*/*Brauer*), (ed. W. A. Herrmann), Georg Thieme Verlag, Stuttgart, 1997, vol. 8, p. 98.
48 F. Abugideiri and R. Poli, in *Synthetic Methods of Organometallic and Inorganic Chemistry* (*Herrmann*/*Brauer*), (ed. W. A. Herrmann), Georg Thieme Verlag, Stuttgart, 1997, vol. 8, p. 102.
49 R. G. Linck, B. E. Owens, R. Poli and A. L. Rheingold, *Gazz. Chim. Ital.*, 1991, **121**, 163.
50 R. Poli, in *Synthetic Methods of Organometallic and Inorganic Chemistry* (*Herrmann*/*Brauer*), (ed. W. A. Herrmann), Georg Thieme Verlag, Stuttgart, 1997, vol. 8, p. 101.
51 J. Andrieu, P. Braunstein and A. D. Burrows, *J. Chem. Res.* (*S*), 1993, 380.
52 Z. Otwinowski and W. Minor, *Methods Enzymol.*, 1997, **276**, 307.
53 G. M. Sheldrick, SHELXS and SHELXL 97, University of Göttingen, 1997.
54 P. Braunstein, M. D. Fryzuk, F. Naud and S. J. Rettig, *J. Chem. Soc.*, *Dalton Trans.*, 1999, 589.
55 A. A. Cole, J. C. Fettinger, D. W. Keogh and R. Poli, *Inorg. Chim. Acta*, 1995, **240**, 355.
56 R. Poli, B. E. Owens and R. G. Linck, *Inorg. Chem.*, 1992, **31**, 662.
57 X. Morise, M. L. H. Green, P. C. McGowan and S. J. Simpson, *J. Chem. Soc.*, *Dalton Trans.*, 1994, 871.
58 R. Felsberg, S. Blaurock, S. Jelonek, T. Gelbrich, R. Kirmse, A. Voigt and E. Hey-Hawkins, *Chem. Ber.*, 1997, **130**, 807.
59 M. V. Galakhov, P. Gomez-Sal, T. Pedraz, M. A. Pellinghelli, P. Royo, A. Tiripicchio and A. Vázquez de Miguel, *J. Organomet. Chem.*, 1999, **579**, 190.
60 J. Andrieu, P. Braunstein, A. Tiripicchio and F. Ugozzoli, *Inorg. Chem.*, 1996, **35**, 5975.
61 J. C. Fettinger, D. W. Keogh, B. Pleune and R. Poli, *Inorg. Chim. Acta*, 1997, **261**, 1.
62 F. Abugideiri, J. C. Gordon, R. Poli, B. E. Owens-Waltermire and A. L. Rheingold, *Organometallics*, 1993, **12**, 1575.
63 C. K. Johnson, ORTEP II, Report ORNL-5138, Oak Ridge National Laboratory, Oak Ridge, TN, 1976.
64 K. Stärker and M. D. Curtis, *Inorg. Chem.*, 1985, **24**, 3006.
65 B. E. Owens and R. Poli, *Inorg. Chim. Acta*, 1991, **179**, 229.
66 F. Abugideiri, D. W. Keogh, H.-B. Kraatz, R. Poli and W. Pearson, *J. Organomet. Chem.*, 1995, **488**, 29.